

Chapter 6: Synthesis of ZnO Nanoparticles

ZnO is a versatile material with an energy gap of 3.37 eV at room temperature. It has been used considerable for its catalytic, electrical, opto-electronic and photochemical properties and applications in transparent electronics, ultraviolet (UV) light emitters, piezoelectric devices, chemical sensors and spin electronics (Nakada et al., 2004; Lee et al., 2005). ZnO is being used as an active channel in invisible thin film transistors, which have achieved much higher field effect mobility than amorphous silicon TFTs (Hossain et al., 2004). These transistors can be widely used for display application. Surface acoustic wave filters using ZnO films have already been used for video and radio frequency circuits. Piezoelectric ZnO thin films have been fabricated into ultrasonic transducers arrays operating at 100 MHz (Ito et al., 1995). On the basis of these remarkable physical properties with the motivation of device miniaturisation, efforts have been focused on the synthesis, characterisation and device applications of ZnO nanostructures such as nanoparticles, nanowires, nanotubes and nanotetrapods. Due to its potential application in nanodevices, ZnO nanostructures, such as nanoparticles, nanorods, nanowires and nanoribbons, have attracted great deal of attention (Taton, 2003). The functional and structural applications of ZnO depend on the peculiar physical properties of exotic nanostructures. Tetrapods shaped whisker shows vibration insulation, microwave absorption, antibacterial effect and antistatic effect (Zhou et al., 2003). Xu and Sun (2003) reported the synthesis of needle-like morphology near the tip, such as nanopins of ZnO for field emitter cathode of high emission efficiency; the nanowires with high aspect ratio has been demonstrated to be good sensors (Wan et al., 2004). In addition, the investigation on ZnO nanostructures helps us to understand the fundamental growth process for the development of novel nanodevices. Different synthesis methods, such as vapour phase transport (VIP) [7,8] metal-organic vapour-phase epitaxy (MOVPE) and CVD [9], dip coating [10], hydrothermal route [11] and electrochemical deposition [12] aqueous thermal decomposition [13] have been reported to fabricate various ZnO nanostructures, such as nanoparticles, nanowires, nanorods, nanoribbon, nanosheet, nanotetrapod, nanobelt, nanodisk, nanowall, nanocage, etc. In the present work, the fabrication and characterisation of ZnO nanoparticles using physical vapour condensation method is reported.

6.1 Experimental

ZnO nanoparticles are synthesised by the physical vapour condensation method. In this method, 99.999% pure zinc pallets used as source material are heated in the presence of oxygen mixed with argon. It is one of the important methods for producing oxide nanostructures at low temperatures. There are some reports on the synthesis of nanomaterials using this method available in the literature [14,15]. Nanostructures synthesised from the metal or alloy using vapour condensation method in the oxygen atmosphere contain some intrinsic defects such as interstitial metallic atom or oxygen vacancies in the oxide nanostructures. These defects have an important effect on the characteristics of the oxide nanostructures. Argon is used as an inert gas in the chamber and its role is to offer the frequent collisions to the atoms of the evaporated materials, which results in the reduction of energy of the evaporated atoms. In this method, the material is typically vaporised into a low-density gas (inert gas) and the vapours move from the hot source to the liquid nitrogen cooled substrate. This

liquid nitrogen cooled substrate is used to enhance the deposition efficiency. The nanoparticles of ZnO are deposited on the substrate and collected in the powder form by scratching from the substrate. For this growth of ZnO nanoparticles, the gas pressure of oxygen and argon is maintained at 5 mbar and 1 mbar respectively. The source material is kept in a molybdenum boat placed at a suitable distance from the substrate. A high vacuum of the order of 10⁻⁶ mbar is maintained in the chamber with the help of diffusion pump attached with the rotary pump. The source material is heated at around 400 C in the presence of these gases to synthesise these ZnO nanoparticles. Powder X-ray diffraction (XRD) is performed using a Philips X-ray diffractometer with Cu K α (1 $\frac{1}{4}$ 1:54178 Å) radiation. The microstructure of these nanoparticles is studied using a transmission electron microscopy (TEM) operated at 100 kV. The UV-VIS absorption spectra is recorded using a V-570 Jasco UV-VIS double-beam spectrophotometer. The scanning wavelength range is 200 nm to 800 nm. In this experiment, we have successfully grown the ZnO nanoparticles at low temperatures, keeping the gases (O₂ and Ar) flow fixed at 5 mbar and 1 mbar respectively.

6.2 Results and discussion

The TEM images of these nanoparticles are presented in Figures 6.1 to 6.4 TEM images reveal the typical morphologies of as-grown ZnO nanoparticles.

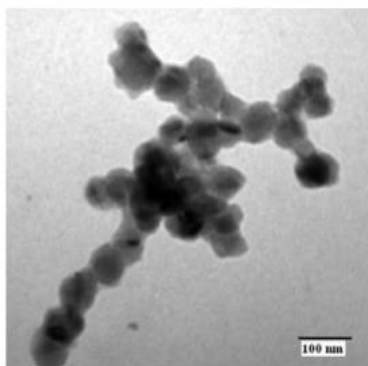


Figure 6.1: TEM IMAGE OF ZnO nanoparticle

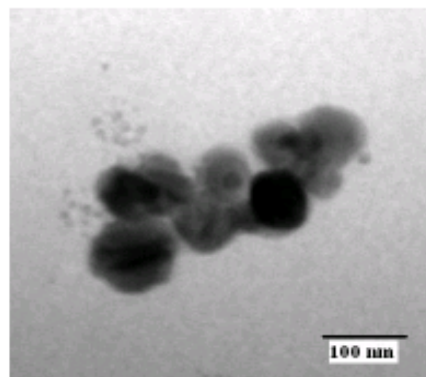


Figure 6.2: TEM IMAGE OF ZnO nanoparticle

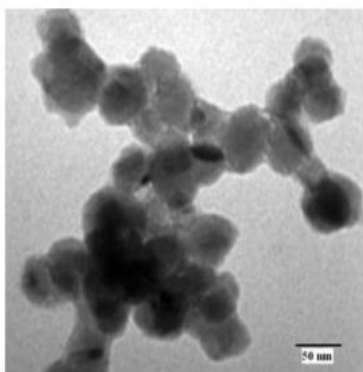


Figure 6.3: TEM image of ZnO nanoparticle

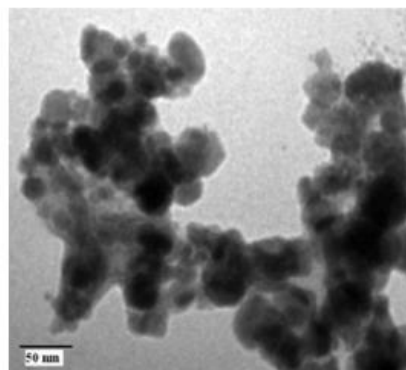


Figure 6.4: TEM image of ZnO nanoparticle

It is observed from these images that the size of these nanoparticles obtained is in the range of 40 nm to 100 nm, but it seems that these nanoparticles contain some impurities and defects. The typical XRD result of these nanoparticles is presented in Figure 6.5. XRD characterization shows that the deposition in the presence of oxygen led to the formation of ZnO nanoparticles. In our process, the source material is heated at 400 C in the presence of oxygen. During this oxidation process the starting material (Zn) is converted into ZnO with a polycrystalline structure. A sharp peak at 36.87 associated with ZnO (101) crystallographic plane is observed. Normally, the diffraction peaks corresponding to (100), (002), (101), (102) and (110) planes are an indication of ZnO with a hexagonal wurtzite structure. These peaks are clearly identified with JCPDS data (JCPDS 36-1451). The intensity of any of these peaks may be higher depending on the preparation conditions of the materials. In our case, the intensity of (101) peak is higher, which clearly demonstrate that the film deposited in oxygen atmosphere has a dominant (101) orientation [16], showing the presence of oxygen vacancies in the so formed ZnO nanoparticles. When the temperature of the melt exceeds its boiling point during resistive heating of the source material i.e. Zn, the smoke consisting of a large amount of embryos above the melt breaks out and spreads out.

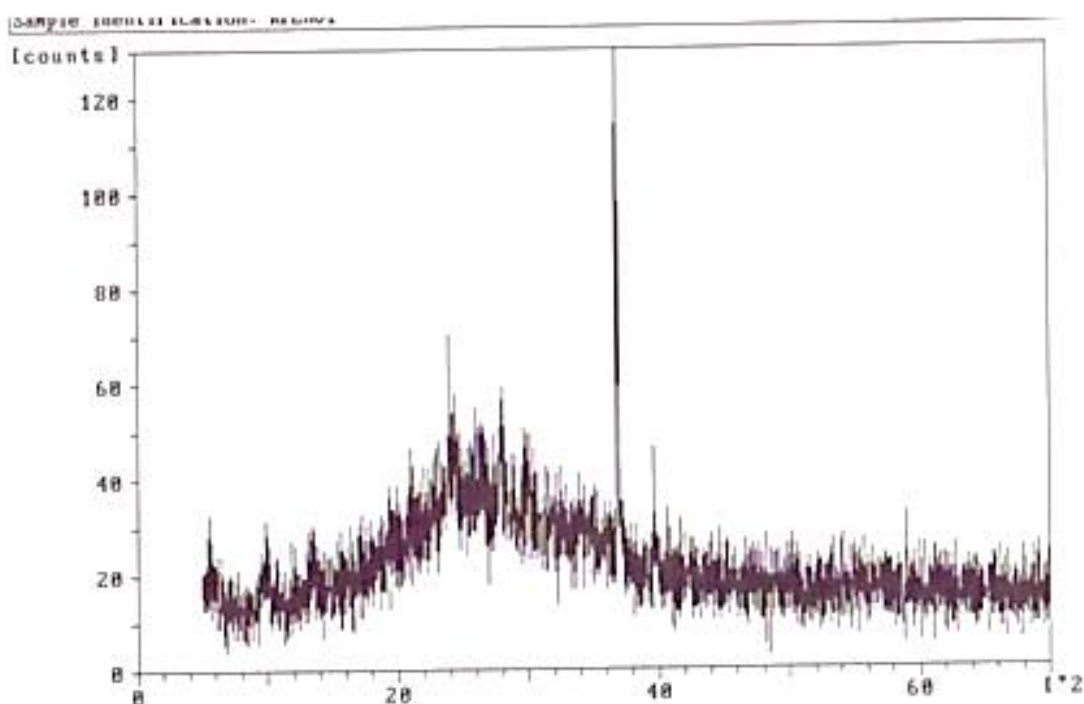


Figure 6.5: XRD spectra of as grown ZnO nanoparticles

An intensive mixing occurs at the interface between the smoke and the mixture gas ambience driven by the convection and then oxidation reaction takes place on the surface of these embryos near the interface. For these embryos, (101) is a preferred growth direction as (101) planes have a high surface energy and preferably absorbs the oxygen atoms for the embryos. The oxidising reaction usually takes place on this coarse prism

surface and forms four protrusions. These protrusions continue to grow by capturing more atoms and finally form the nanoparticles to minimise their interface energy. The growth mechanism of these ZnO nanoparticles in the inert gas condensation process includes nucleation, particle growth, particles coagulation and coalescence. The processing condition decides the role played by any of these mechanisms on the characteristics of as grown nanoparticles. The process involves the effusion of atoms from the source material and these atoms will rapidly lose their energy by colliding with gas atoms. As the collision mean free path is very short, the nucleation process is performed homogeneously in the vapour phase. The nucleation begins abruptly and proceeds at a very high rate as the difference between the evaporation temperature and the gas phase is very high. For example, an under cooling of 400 K at the evaporation temperature of 1297 K results in a supersaturation value of the order of 105. According to Yang et al. (2002), the nucleation process is considered negligible when supersaturation exceeds 106. An under cooling of the order of few hundred degrees leads to the formation of nanoparticles as the critical diameter of embryonic particles and the nucleation energy barrier are extremely low. These particles serve as sink for additional vapour and quickly reduce the supersaturation, which results in the quenching of additional nucleation. If the supersaturation is limited, the rate of particle formation would be reduced, leading to lower initial number concentrations. The nucleuses can then grow to larger size as additional material is deposited on the surfaces of the growing particles. The distribution of the nanoparticle size must be narrow as reported by Okuyama et al. [17] and Flagan and Lunden [18] as the relative range of particle sizes will decrease during growth. In the present system, narrow particle size distribution was not obtained. Therefore, the supersaturation and thus nucleation are very high. In this case, the particle growth had to be performed due to Brownian coagulation, i.e., the collision of nucleuses resulted in particle growth. The present growth mechanism involves the vapourisation of material into allowed density gas by resistive heating and the vapours migrate from the hot source to liquid nitrogen cooled substrate. The decrease in the evaporation temperature leads to a far more rapid decrease in the equilibrium vapour pressure and correspondingly high supersaturation (Granqvist and Buhrman, 1976). At high supersaturation, the vapours rapidly nucleate, forming very large numbers of extremely small particles. The particles then grow by Brownian coagulation (Snikta et al., 2007). Figure 6.6 shows the room temperature absorption spectra of as-grown ZnO nanoparticles.

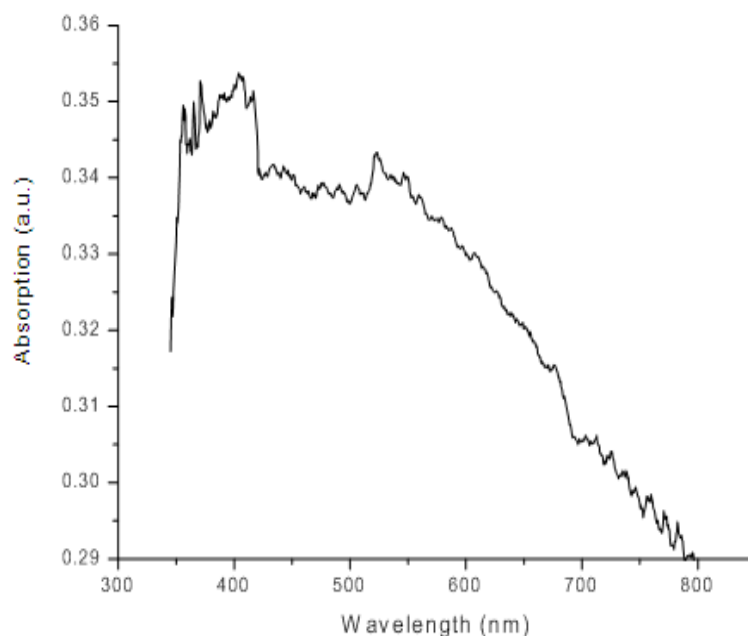


Figure 6.6: UV visible spectra of as grown ZnO nanoparticles

The absorption spectra have a very narrow peak near the band edge in the exciton absorption region (at about 381 nm) and red-shifted relative to the bulk exciton absorption (373 nm). From the absorption spectra, one can see that there is absorption almost in the whole violet and visible region. The band edge absorption begins with the wavelength at ~ 800 nm suggesting that more absorption states or defect energy bands exist in this sample, which agrees well with the discussion on the formation mechanism of these nanoparticles. Moreover, the broad peak at 373 nm may be associated with the presence of oxygen in as grown ZnO nanoparticles (Nan et al., 2005). This broad peak is accounted for the conversion of Zn into ZnO, which corresponds well with the XRD data. The UV-VIS absorption spectra of these nanoparticles also show a typical behaviour between 400 nm and 500 nm. This may be attributed to oxygen vacancies/defect levels in the band gap, which have an important effect on the characteristics of these zinc oxide nanoparticles. Due to the excellent optical properties, these nanoparticles grown at low temperatures are quite interesting for device applications.

6.3 Conclusions

These nanoparticles of ZnO are grown at a low temperature of 400 C using a simple technique. These nanoparticles are almost spherical in shape and the size varies from 40 nm to 100 nm. The XRD spectra shows a broad peak at 36.87, which confirms the growth of ZnO nanoparticles. From the absorption spectra, a broad peak at 373 nm is accountable for the conversion of Zn into ZnO, which agrees fairly with the XRD result. The growth mechanism of these nanoparticles involves the vaporisation of material into a low-density gas by resistive heating and the vapours migrate from the hot source to liquid nitrogen cooled substrate. The decrease in the evaporation temperature leads to rapid decrease in the equilibrium vapour pressure and correspondingly high supersaturation. At high supersaturation, the vapours rapidly nucleate, forming very large numbers of small particles. These small particles then grow by Brownian coagulation.

6.4 References

- [1] Nakada, T., Hirabayashi, Y., Tokado, T., Ohmori, D. and Mise, T. (2004) 'Novel device structure for Cu (In,Ga) Se₂ thin film solar cells using transparent conducting oxide back and front contacts', *Sol. Energy*, Vol. 77, pp.739–747.
- [2] Lee, S.Y., Shim, E.S., Kang, H.S., Pang, S.S. and Kang, J.S. (2005) 'Fabrication of ZnO thin film diode using laser annealing', *Thin Solid Films*, Vol. 473, pp.31–34.
- [3] Hossain, F.M., Nishii, J., Takagi, S., Sugihara, T., Ohtomo, A., Fukumura, T., Koinuma, H., Ohno, H. and Kawasaki, M. (2004) 'Modeling of grain boundary barrier modulation in ZnO invisible thin film transistors', *Physica E*, Vol. 21, pp.911–915.
- [4] Ito, Y., Kushida, K., Sugawara, K. and Takeuchi, H. (1995) 'A 100-MHz ultrasonic transducer array using ZnO thin films', *IEEE Trans. Ultrasonics, Ferroelectrics and Frequency Control*, Vol. 42, pp.316–324.
- [5] Taton, T.A. (2003) 'Bio-nanotechnology: two-way traffic', *Nature Mater.*, Vol. 2, pp.73–76.
- [6] Zhou, L. Lu, D. L. Zhang, Z. W. Pan and S. S. Xie, "Linear conductance of multiwalled carbon nanotubes at high temperatures", *Solid State Communications* 129 6 407 (2004).
- [7] Fei, L., Zhen, L. and Fujiang, J. (2008) 'Fabrication and characterization of ZnO micro and nanostructures prepared by thermal evaporation', *Physica B*, Vol. 403, pp.664–669

-
- [8] Haiping, T., Zhizhen, Y., Liping, Z., Haiping, H., Binghui, Z., Yang, Z., Mingjia, Z. and Zhixiang, Y. (2008) 'Synthesis of radial ZnO nanostructures by a simple thermal evaporation method', *Physica E*, Vol. 40, No. 3, pp.507–511.
- [9] Mitra, S., Sridharan, K., Unnam, J. and Ghosh, K. (2008) 'Synthesis of nanometal oxides and nanometals using hot-wire and thermal CVD', *Thin Solid Films*, Vol. 516, No. 5, pp.798–802.
- [10] Sasani Ghamsari, M. and Vafaei, M. (2008) 'Sol-gel derived zinc oxide buffer layer for use in random laser media', *Materials Letters*, Vol. 62, Nos. 12–13, pp.1754–1756.
- [11] Sifei, S., Peijun, J., Shengchun, L. and Wei, B. (2008) 'Stable field emission from rose-like zinc oxide nanostructures synthesized through a hydrothermal route', *Materials Letters*, Vol. 62, Nos. 8–9, pp.1200–1203.
- [12] Ravi, C. and Raychaudhuri, A.K. (2008) 'Electrodeposition of aligned arrays of ZnO nanorods in aqueous solution', *Solid State Comm.*, Vol. 145, Nos. 1–2, p.81.
- [13] Shisheng, L., Haiping, T., Zhizhen, Y., Haiping, H., YuJia, Z., Binghui, Z. and Liping, Z. (2008) 'Synthesis of vertically aligned Al-doped ZnO nanorods array with controllable Al concentration', *Materials Letters*, Vol. 62, Nos. 4–5, pp.603–606.
- [14] Turker, M. (2004) 'Effect of production parameters on the structure and morphology of Ag nanopowders produced by inert gas condensation', *Mater. Sci. Engg. A*, Vol. 367, pp.74–81.
- [15] Lehtinen, K.E.J. and Zachariah, M.R. (2002) 'Energy accumulation in nanoparticle collision and coalescence processes', *J. Aerosol Sci.*, Vol. 33, pp.357–368.
- [16] Reetz, M.T. and Helbig, W. (1994) 'Size-selective synthesis of nanostructured transition metal clusters', *J. Am. Chem. Soc.*, Vol. 116, pp.7401–7402.
- [17] Okuyama, K., Kousaka, Y., Toghe, N., Yamamoto, S., Wu, J.J., Flagan, R.C. and Seinfeld, J.H. (1986) 'Production of ultra-fine metal oxide aerosol particles by thermal decomposition of metal alkoxide vapors', *AIChE J.*, Vol. 32, pp.2010–2019.
- [18] Flagan, R.C. and Lunden, M.M. (1995) 'Particle structure control in nanoparticle synthesis from the vapor phase', *Mater. Sci. Engg. A*, Vol. 204, p.113.
- [19] Granqvist, C.G. and Buhrman, R.A. (1976) 'Ultrafine metal particles', *J. Appl. Phys.*, Vol. 47, No. 5, pp.2200–2219.
- [20] Snikta, V., Jankauskas, V., Zunda, A. and Mizariene, V. (2007) 'Deposition of nanocrystalline ZnO by wire explosion technique and characterization of the films' properties', *Materials Letters*, Vol. 61, pp.1763–1766.
- [21] Nan, P., Wang, X., Ghang, K., Hailong, H., Xu, B., Fanking, L. and Hou, J.G. (2005) 'An approach to control the tip shapes and properties of ZnO nanorods', *Nanotechnology*, Vol. 16, pp.1069–1072.